Final Report for NASA grant NAGW-4064

Prepared by: Dr. Dennis Gallagher
Ball Aerospace and Technologies Corp.
P.O. Box 1062 Mail Stop T-3
Boulder, CO 80306-1062
Phone: (303) 939-4567
Email: dgallagher@ball.com

Sub-Arcsec X-ray Telescope for Imaging the Solar Corona in the 0.25-1.2 keV Band (Final Report of NAGW-4064)

The primary focus of this research was to build and test an X-ray telescope using spheres at grazing incidence. Three test runs at the High Energy Laser Systems Test Facility (HELSTF) were made. The results for the first two runs were written up and presented at an SPIE conference July, 1996. A copy of the paper presented at this conference follows. The basic concepts, problems, and solutions encountered in this study are described in this paper.

Sub-arcsec x-ray Telescope for Imaging The Solar Corona In The 0.25-1.2 keV Band

Dennis Gallagher
Ball Aerospace and Technologies Corp./University of Colorado, CASA
Boulder, Colorado 80306

Webster Cash, Schuyler Jelsma, Jason Farmer
University of Colorado, CASA
Boulder, Colorado 80309

ABSTRACT

We have developed an x-ray telescope that uses a new technique for focusing x-rays with grazing incidence optics. The telescope was built with spherical optics for all of its components, utilizing the high quality surfaces obtainable when polishing spherical (as opposed to aspherical) optics. We tested the prototype x-ray telescope in the 300 meter vacuum pipe at White Sands Missile Range, NM. The telescope features 2 degree graze angles with tungsten coatings, yielding a bandpass of 0.25-1.5 keV with a peak effective area of 0.8 cm^2 at 0.83 keV. Results from x-ray testing at energies of 0.25 keV and 0.93 keV (C-K and Cu-L) verify 0.5 arcsecond performance at 0.93 keV. Results from modeling the x-ray telescope's response to the Sun show that the current design would be capable of recording 10 half arcsecond images of a solar active region during a 300 second NASA sounding rocket flight.

Keywords: X-ray optics , Grazing Incidence, Solar physics

1. INTRODUCTION

Resolution of grazing incidence x-ray optics has usually been limited by scattering from surface figure errors. X-ray telescope designs typically have highly aspherical surfaces that are very difficult to polish smooth due to the fact that polishing laps can contact only a small region of the optical surface at a time. Great efforts have gone into fabrication of grazing incidence optics (such as the AXAF mirrors) with reduced mid-frequency errors. Because x-ray optics use graze angles of a few degrees or less, mid-frequency errors translate into surface topography errors with scale lengths on order 1-25 mm. It is diffraction from these surface errors that scatters x-rays in the few arcsec range.

To achieve resolution significantly below an arcsecond requires a surface smooth to $\lambda/200$ or even $\lambda/500$ (rms) at 6328 Å on scale lengths of 1 to 25 mm.

Current optical fabrication techniques routinely polish optical flats, spheres, and slightly apsherical (normal incidence) optical surfaces to $\lambda/200$ across apertures far greater than 25 mm. That is to say, if these optics could be used in the design of an x-ray telescopes, their surface quality would allow x-ray imaging performance of 0.1 arcsec or better. We are currently developing such a telescope, using spherical optics at grazing incidence.

In this paper we discuss some of the basic theory and concepts of how the grazing incidence spherical telescope works, and present test results from the first full scale telescope.

2. SPHERES AT GRAZING INCIDENCE

We start with a conventional spherical mirror and assume it is roughly square in its dimensions. When tilted over to a typical graze angle of a few degrees, it presents a long, narrow entrance aperture. For the sake of clarity, let us assume that is roughly 30 cm across. This makes the entrance aperture 30 cm long and 1 cm wide.

If the mirror is concave, it will provide a low quality focus at a distance of Rsin(θ)/2 where R is the radius and θ the graze angle. If we desire a typical focal length of 2 meters, R must be about 100 meters. The focus will be very nearly a straight line, since the curvature in the other direction is only a few microns over the entire 30 cm length. In other words, the sphere is nearly indistinguishable from a cylinder in optical terms. Similarly, because this is an f/300 sphere, the spherical surface is nearly indistinguishable from a paraboloid. Thus pure spheres are used throughout the design.

The quality of this focus is poor, typically in the range of a few minutes of arc, so it has never been used for astronomy. Second, the focal surface lies along a grazing incidence Rowland circle, making the field of view small.

The principal drawback to single spheres is the poor quality of the. The deviation of the spheres from the grazing paraboloid is simply too great, as shown schematically in Figure 1.

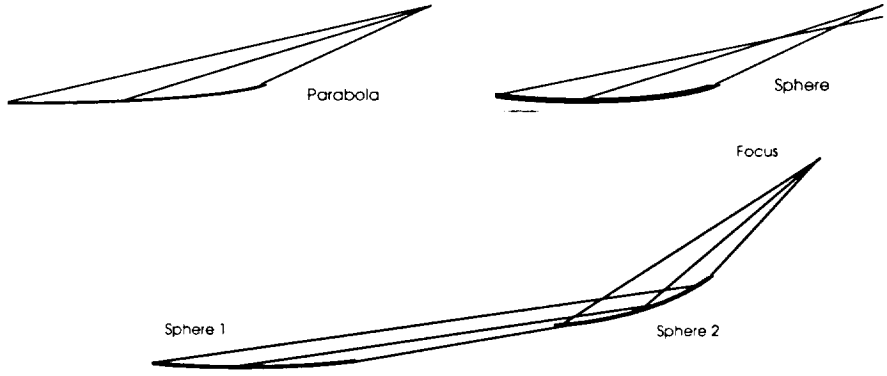

Figure 1: Above (left) is a schematic of a grazing incidence parabola of the kind used in Wolter telescopes. Parallel light is focused to a perfect point. Above (right) is the equivalent diagram for a sphere used at grazing incidence. There is a severe comatic aberration that limits the resolution. The bottom diagram shows schematically a two sphere layout that produces a high quality line focus.

Another sphere, properly positioned and oriented relative to the first sphere, can correct the severe comatic aberration, removing it entirely and leaving spherical aberration as the dominant source of blur. The discovery of this design class and the supporting analysis are reported by Cash (1996). Entire classes of geometries exist, analogs of the Wolter Types I, II and III.

The quality of the line focus thus formed came as a surprise. Many practical geometries turned out to have 0.1 or even 0.01 arcsec imaging on axis. Indeed, the quality of focus was below the diffraction limit for many applications, since a 20 Å beam across a 1 cm aperture is diffraction limited at about .05". When the effects of scattering on a high quality sphere at grazing incidence are calculated, one again finds that standard numbers predict a scattering limit in the neighborhood of 0.1". In other words, for the first time, we have a practical means to fabricate diffraction limited x-ray optics!

The two sphere telescope images in only one dimension but, like the Kirkpatrick Baez telescope, another pair of optics can be place orthogonal to the first pair to produce a two dimensional focus. Figure 2 shows schematically how the optics are positioned to produce a two dimensional focus. One slight draw back to this design is the final focus results from a minimum of four reflections. The spheres can be thought of as simple lenses where their focal length is determined by the relation $f=R\sin(\theta)/2$.

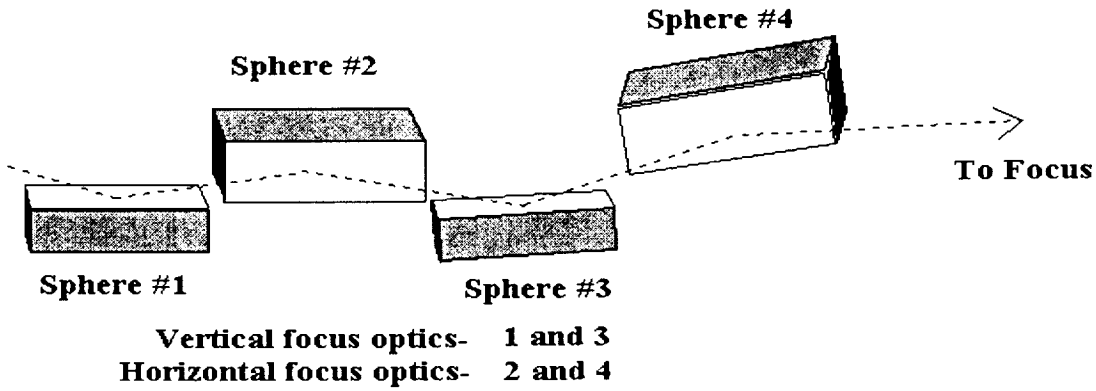

Figure 2: A schematic lay out of a four sphere telescope that produces a high quality 2-D focus. Our spherical telescope uses all concave spheres laid out in this fashion. This arrangement is an analog of the Wolter Type-I telescope.

3. THE SPHERICAL X-RAY TELESCOPE DESIGN

3.1 Design

As previously discussed, there is a large family of solutions for the Spherical Telescope (ST) design. We chose a design for our first ST where the first four spheres are concave, located next to each other, and have approximately 2° graze angle reflections. The geometric aperture for ST is one centimeter square, making the spheres 290 mm

long. As in Figure 2, the reflective surfaces alternate in a cross pattern where the first surface is 0° and the next surface is flipped 90° to the first, continuing for the four spheres. The pair of spheres at 0° focuses an image in one direction and the pair at 90° image in the orthogonal direction which results in a 2-D image with an effective focal length of 2.7 meters for ST. The exact angles and radii for the ST spheres were calculated by raytrace optimization and are shown in Table I. The first focus is then magnified by a pair of relay optics to an effective focal length of ~10 meters or ~20 meters depending on which relay optics we use. The first relay optic is convex and is placed inside the first focus analogous to the Cassegrain design. The second relay optic is concave and placed past the first focus, analogous to the Gregorian design. Their placement and radii were determined by the equation $1/f = 1/d1 + 1/d2$ where $f=R\sin(\theta)/2$. Raytrace optimization was also used to find the best radii for the spherical relay optics. The magnified image reduced off-axis aberrations in most cases. We believe this to be an effect of field flattening. The main purpose for the relay optic system is to magnify the plate scale to match the pixel size of our CCD camera.

Table I Spherical Telescope Parameters (10 meter EFL design)

Element (mm)	Radius (mm)	Separation	Angle (deg)	Comment
Sphere 1	+241400.	0.	1.96240	Focus in X direction
Sphere 2	+218700.	300.	1.94238	Focus in Y direction
Sphere 3	+434900.	300.	1.98088	Correct in X direction
Sphere 4	+380580.	300.	1.97615	Correct in Y direction
Relay	-7000.	2053.310	1.51852	Y direction relay optic
Relay	+3000.	2168.310	1.38914	X direction relay optic
Plane	∞	2364.310	na	focal plane

3.2 Optics

The four large spheres are made from fused silica and are 290 mm long, 25 mm wide, and 50 mm thick and were fabricated by Zygo Inc., of Middlefield, CT. The spherical relay optics are 50 mm diameter and were purchased directly from CVI Laser Inc., of Albuquerque, NM. No special super polishing techniques were used to make any of the spheres. Both the Zygo and CVI Laser spheres had their surfaces measured with a Wyko interferometer and all have a fine surface finish of 5 Å RMS (0.6 mm scale). Measurement of the radii of the four long radii spheres to better than 1% was required so metrology could be used to align the ST for 0.5 arcsec imaging. This posed a challenge because the spheres were too long to measure directly on an optical rail and they were to short to measure directly referenced to an optical flat. We developed a test procedure where the spheres were placed in an auto-collimated setup using an optical flat. The difference in null (focus) off the long radii sphere and the flat were measured to give the radii of each sphere to a very high accuracy ~0.5%. We also had the long radii surfaces characterized by profilometry at the Brookhaven National Laboratories by Dr. Peter

Tackus to provide an extra check to our radius measurements. Both measurements agreed to within error bars

The optics for the ST telescope were coated with tungsten by Hyperfine, Boulder CO. Tungsten provides excellent reflectivity in the 0.25-1.25 keV range. This was verified using Henke (1993) tabulated optical constants. We also measured the reflectivity of glass samples coated with 500 Å of tungsten from 0.25-1.5 keV and our measurements were in excellent agreement to the Henke data. Another interesting advantage of using tungsten is that the coatings are extremely durable and can not be scratched or removed by aluminum oxide pitch polishing. The coatings also pass a tape pull test. This is a very important advantage when the optics have to be in the field for laboratory testing or for a rocket flight.

3.3 Test Telescope Structure

A photo of the ST structure is shown in Figure 3. The camera utilizes a thinned back-illuminated CCD chip (model SI502A) from Scientific Imaging Technologies of Beaverton, OR. The PC based CCD electrical system was developed by Ball Aerospace of Boulder, CO.

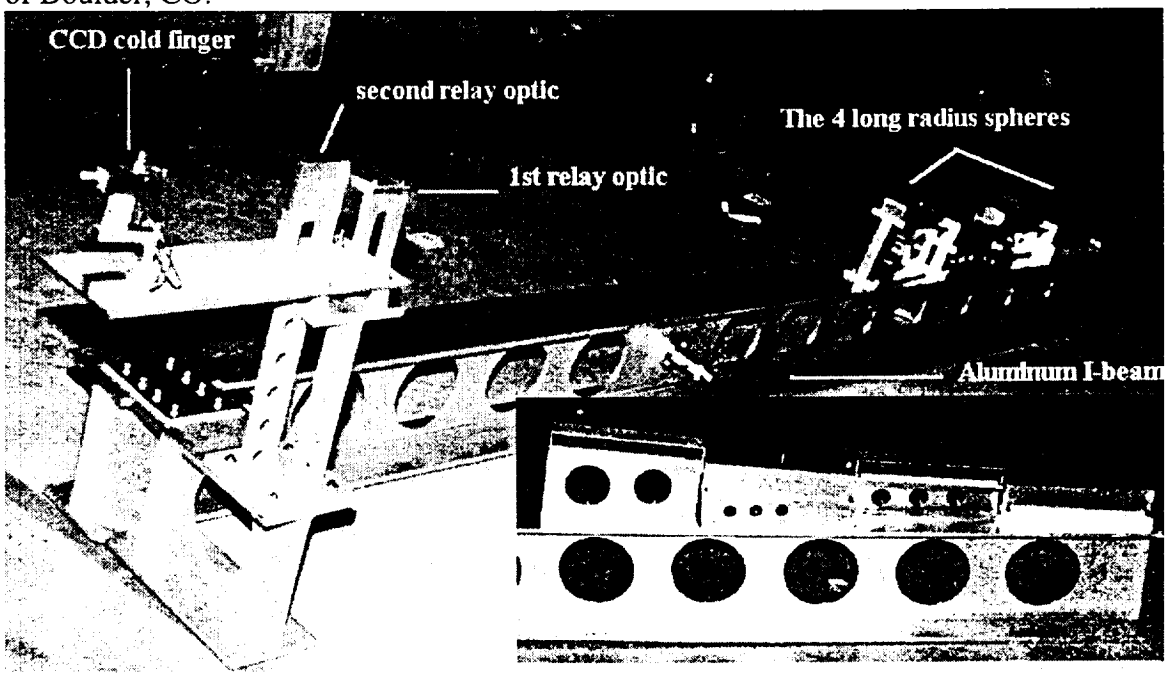

Figure 3: The main part of the structure is a 10" wide I-beam, 9 feet long, made of 6061 aluminum. The four 290 mm long by 25 mm wide ST spheres and their mounts are seen at the far end of the beam. The pedestal at the left has the relay optics and CCD detector cold finger mounted on it. The inset shows a close up of the long radii spheres and their mounts. We built two relay optic sections giving 10 and 20 meter ST effective focal lengths, or 0.50 arcsec and 0.33 per 27μ pixel plate scale in each design respectively.

3.4 Assembly and Alignment

The alignment tolerances of the four elements are remarkably loose, given the quality of the image. This is predominantly the effect of the very slow nature of the beam, ≈ f/300. The tightest position tolerance between any two elements of the system is ±0.3 mm. The tightest angular constraint is ±15 arcsec. We aligned our systems using a collimated light source to illuminate all the optics. We then raytraced the final reflection off of each optic back 40 feet to a flat wall. As the optics were placed in position, the reflected light off the optic was made to strike the wall at the position that the raytrace code predicted. The accuracy that the optics can be aligned by this method is about ±15 arcsec which is sufficient to realize sub-arcsec performance.

3.5 Raytrace results of 10 meter EFL Spherical Telescope

In Figure 4 are spot diagrams obtained by raytracing the 10 meter spherical telescope design given in Table I. The field over which ST maintains sub-arcsec imaging is small; 0.5 arcsec imaging is maintained across about 30 arcsec. The field of view is roughly 60X60 resolution elements. In other words 2 arcsec resolution is maintained across a 2 min of arc diameter field for this 10 meter ST. Larger field ST designs are possible at the expense of including extra reflections.

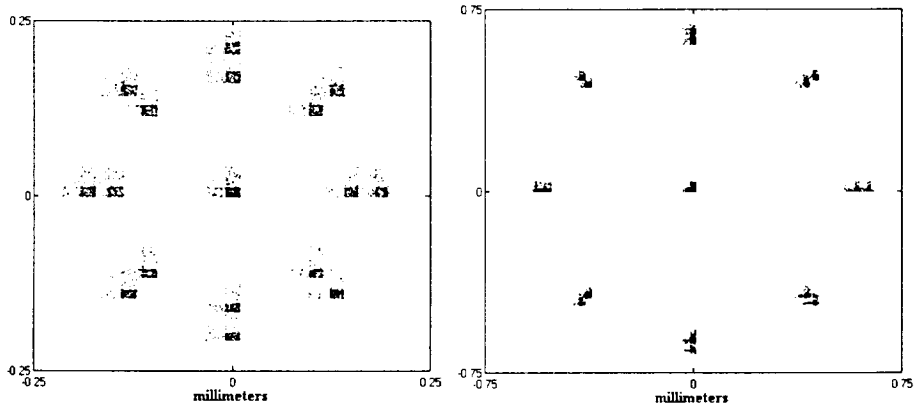

Figure 4: The raytrace at (left) simulates an on axis point source surrounded by point sources placed every 45 degrees in azimuth on radii of 4 and 5 arcsec. The raytrace on the (right) is the same except the radii are 15 and 16 arcsec. Both object distances are 300 meters. The design gives similar results at infinity, but the optics needs angle corrections on the order a few minutes of arc.

Figure 5 shows a raytrace simulation design to show the field of few and the slight distortion in the magnification at off-axis angles. The distortion is mainly caused by the relay optics and can be virtually eliminated if we choose to use custom radii for the two relay spheres.

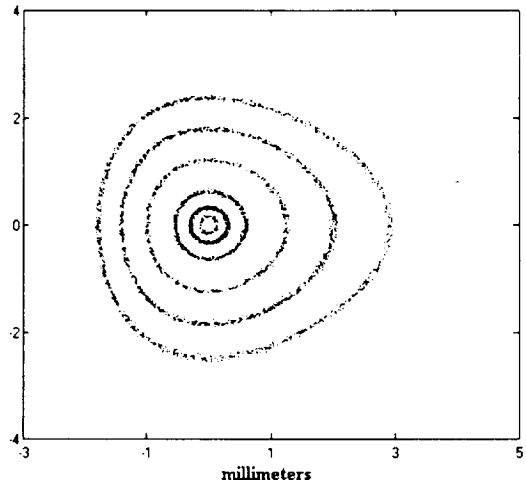

Figure 5: Rings 1 arcsec wide at radii of 1.5, 5.5, 10.5, 21.5, and 30.5 arcsec at 300 meters.

4. TEST AT THE HELSTF LONG PIPE FACILITIES

4.1 HELSTF Facilities

We have tested the spherical telescope at the High Energy Laser System Test Facility (HELSTF) in White Sands New Mexico twice and, as of this writing, are preparing to test again in a few weeks. HELSTF has unique facilities for testing x-ray systems and has participated in calibrations of flight instruments such as the Soft X-ray Telescope (SXT) on the Yohkoh satellite, the ASTRO-E engineering telescope, and five University of Colorado rocket instruments. A schematic of our HELSTF test setup is shown in Figure 6. The test setup centers around a 300×0.61 m diameter vacuum pipe. A source of x-rays comes from one end and the test telescope is 300 meters away at the other end of the pipe. We collected data at 44.7 Å (C-K) and at 13.3 Å (Cu-L).

The x-ray source for this test has some unique features. A J.E. Manson soft x-ray source is placed on a X-Y-Z stage at the focus of a 218 mm diameter F/5.7 Wolter 1.25° degree graze angle telescope. The telescope was fabricated for an earlier sounding rocket experiment (Gallagher, 1990, 1991). The telescope quasi-collimates the x-rays down the 300 m vacuum pipe to a vacuum test chamber which contains the test telescope. The collimator telescope serves two purposes. First, it concentrates the x-ray flux at the vacuum test chamber by a factor $\sim 10^6$ over that of just the open source. Second, target test patterns placed at the front of the collimator are back illuminated with x-rays creating objects for imaging that are not blurred by the arcmin figure quality of the collimator. The Manson source emits x-rays from a point approximately 1 mm in diameter or 0.75 arcsec at 300 meters. This would make it difficult to test 0.5 arcsec imaging if used alone without the collimator. The x-ray source is filtered with 2000 Å of polyimide and 500 Å of aluminum for 44.7 Å measurements, and with 2000 Å polyimide and 2000 Å of copper for 13.3 Å measurements. The test telescope was designed to focus at 300 meters on the target patterns placed in front of the collimator. The optics for the collimator only serve to back illuminate the target patterns with x-rays, hence the minute of arc quality

collimator figure does not affect the sub-arcsec response of the ST. A better name for the collimator might be an "x-ray concentrator". The finite size of the source and figure errors on the Wolter telescope serve to spread the x-rays which allows for complete illumination of the 1 cm ST pupil. The ST structure is driven on an altazimuth mount by micro positioning Klinger stages for making pointing adjustments while under vacuum. Figure 7 shows the test telescope in the vacuum chamber and the collimator exit aperture plate at the other end of the 300 meter pipe.

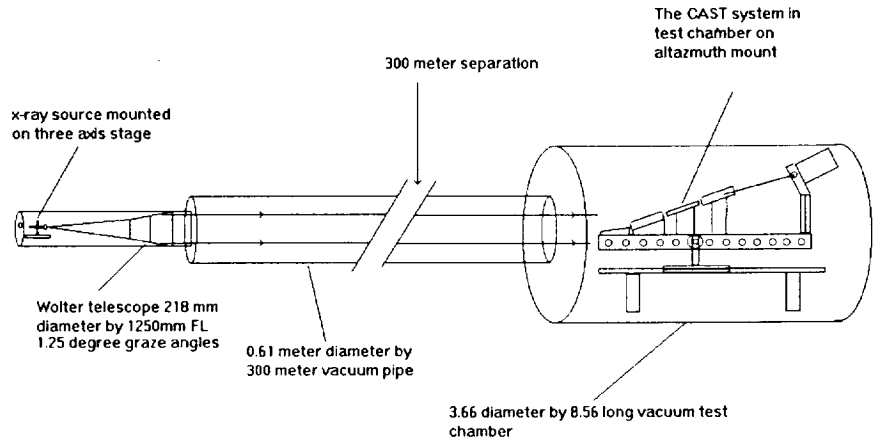

Figure 6: Schematic of the HELSTF test setup used to collect sub-arcsec quality images with ST. The complete chamber is pumped using a 48" cryo pump which brings the entire system to about 5×10^{-6} *Torr.*

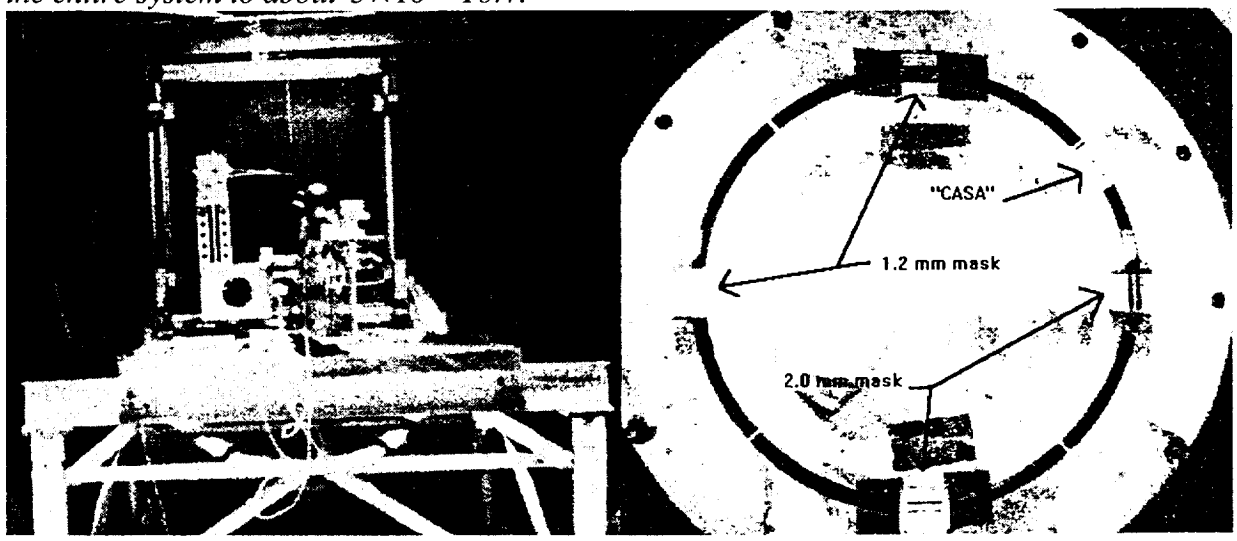

Figure 7: Test setup at HELSTF. To the (left) is the telescope inside the vacuum chamber. In the background is the Klinger positioning device used to move the telescope on its altazimuth mount. To the (right) is the collimator pupil at the other end of the 300 meter

pipe. The collimator was originally built for a sounding rocket flight and the structure is still housed in the standard 17" diameter rocket skin. The exit aperture plate of the collimator has a 8 mm wide annulus with a diameter of 226 mm. The object test patterns can be seen mounted to the aperture plate. One set of masks has 2 mm bars (1.4 arcsec) placed at orthogonal locations on the aperture plate and another set has 1.2 mm bars (0.8 arcsec) also orthogonal. The bars are ~25 mm long. Also shown is a mask with ~5 mm letters spelling "CASA".

4.2 X-ray Data

As of this writing we have done two test runs at the HELSTF facilities and are currently planning a third run in mid June 1996. Results from our first HELSTF tests demonstrated that the ST imaging capabilities were better than 1 arcsec, but the data were flawed by double images caused by a mis-aligned relay optic. This relay optic used two spheres attached to each other at 90 degrees forming a "V" shaped optic. The x-rays from the four main spheres fell along the apex of the "V" shaped optic. A slight twist in the alignment of the "V" resulted in double images. For our second HELSTF run we developed a new relay system that uses the convex and concave spheres described earlier. This relay system eliminates the possibility of double images and are much easier to align. The results from our second HELSTF test, with the new relay optic, were significantly improved, but we later found that we had a coupled 5 min of arc error on the alignment between the two long radii spheres imaging in the horizontal direction. The result of this error was a 30 arcsec blur in the horizontal imaging direction. The horizontal imaging direction was extremely sharp and resolved to better than 0.5 arcsec. Figure 8 shows an image from our last data run and a raytrace simulating the mask and the 5 min of arc angle error.

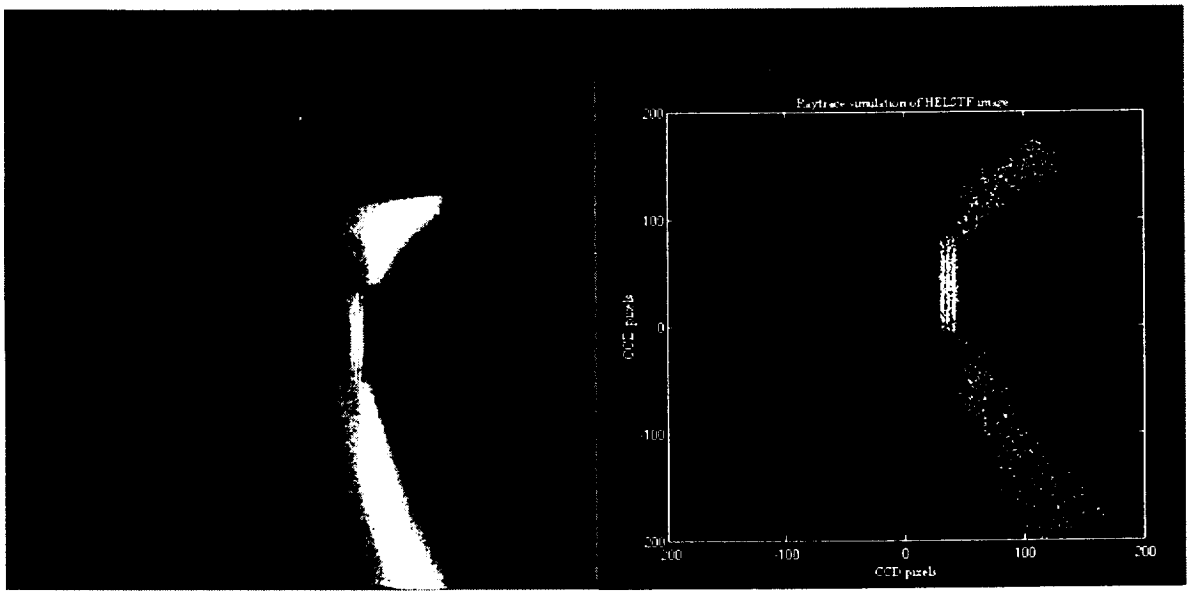

Figure 8: To the (left) is an image taken with 0.93 keV (Cu-L) x-rays of the 1.2 mm mask using the 20 meter EFL relay optical system. The image shows better than 50%

modulation at 0.8 arcsec. To the (right) is a raytrace simulation of the ST imaging the 1.2 mm mask. The 30 arcsec blur is in the vertical direction as seen in these images.

The image in Figure 8 was taken with the cryo vacuum pump motors off and the liquid nitrogen to the CCD was temporarily turned off to eliminate possible sources of vibrations. This image shows a definite improvement over the previous data we collected with the sources of vibration turned on. For example, the intensity at the sharp edge on the right side of the mask in the image of Figure 8 falls to below 50% intensity in one CCD pixel or 0.33 arcsec.

5. MODELING TELESCOPE RESPONSE TO THE SOLAR CORONA

One immediate use of the single channel small aperture ST is to use it to image fine filamentary structure in the solar corona over active regions in the x-ray with unprecedented spatial resolution. Because ST employs grazing incidence optics it would be capable of imaging the corona at energies greater than that possible using the normal incidence multilayer techniques (Golub,1982,1989,1990; Hoover,1990; Walker 1988). Also, the ST would not be bandwidth limited like instruments employing the multilayer technique allowing use with spectroscopic instruments. Figure 9 shows an effective area plot of the current ST. The computation of the effective area of ST is based on theoretical optical constants and actual measurements of various components. The peak of this curve is about 0.08 cm^2 at 13Å.

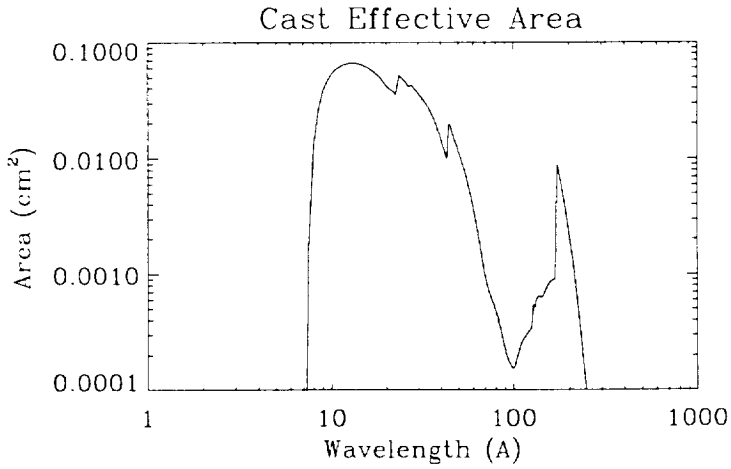

Figure 9: The effective area of ST. The plot was derived from Henke (1982) data adjusted to fit measured data for transmission and reflections. A filter of 1000 Å Lexan, 1000 Å Al, and 200 Å Ti to block out of band solar radiation was included in the model. A model for a thinned back illuminated CCD QE was also used.

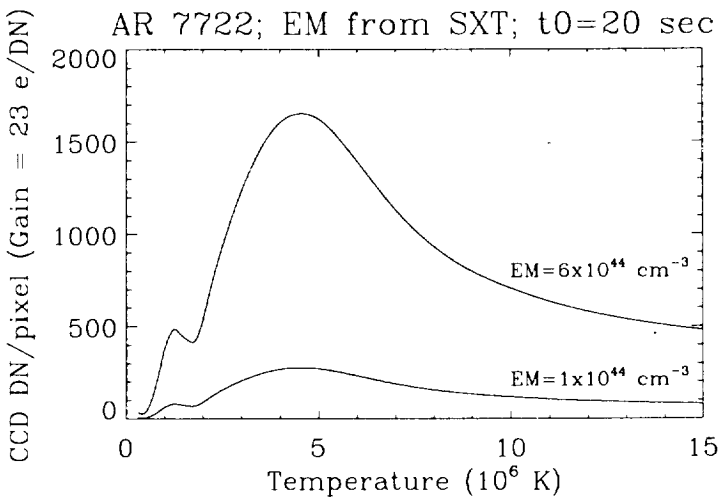

Figure 10: The predicted ST signal for the brightest portion and the 50% level contour of Active Region 7722. The assumed pixel size is 0.5×0.5 *arcsec. Note that a typical active region may be easily observed in a 20-sec exposure.*

The predicted signal through the ST at the CCD was computed and is shown in Figure 10. The model was constructed by convolving theoretical solar spectra with the instrument response curve. The theoretical spectra were computed from the results of Mewe et al. (1985, 1986). For the predicted signal we have assumed an observing time of 20 sec, 0.5×0.5 arcsec pixels, and volume emission measure ($EM = \int n_e^2 \, dV$; n_e = electron density; dV = the emitting volume) values as measured by SXT from its 2.45×2.45 arcsec pixels. For this particular active region, the peak intensity in the SXT image gives $EM = 6.\times 10^{44}$ cm^{-3} and the 50% integrated count level contour gives $EM = 1.\times 10^{44}$ cm^{-3}. The measured SXT temperatures are between 3×10^6 K and 3.5×10^6 K. One can see from the simulation that a good signal level is obtained with the ST in a 20 second exposure. A NASA rocket's attitude control system should be able to maintain better than 0.5 arcsec pointing stability for about 1 minute and 3 arcsec over the total 5 minute observation period (Welch private communication).

6. CONCLUSION

We have demonstrated a new type of x-ray telescope that overcomes the difficulties associated with polishing highly aspheric optics to super smooth surfaces. The cost of the spherical optics is a small fraction of the cost of polishing highly aspheric optics. The collecting area of the ST can be greatly increased by nesting the spheres in a manner analogous to the Wolter telescopes. Current off-the-shelf, spherical optic polishing techniques should yield STs with 0.1 arcsec resolution capability. With state of the art polishing techniques we believe that the STs could be fabricated to resolve at 0.01 arcsec and beyond.

We are currently planning to return to the HELSTF facilities to test our current ST to 0.1 arcsec. We have constructed new relay optics that will magnify the first focus to 50 meters EFL. To achieve 0.1 arcsec resolution, we had to reduced the aperture of the ST to 0.5X0.5 cm. This telescope could be used to study solar flares, the brightest sources of extra terrestrial x-rays, with resolution an order of magnitude better than any current x-ray telescope.

The authors would like to thank Don Hillis of Ball Aerospace for his help in developing an operational CCD camera system. Thanks are also due to Dr. Peter Tackus for measuring the long radii spherical optics and to Dr. James Lemen of Lockheed for his work in modeling the ST response to the solar corona and providing comparisons to SXT data. This work was supported by NASA grants NAGW-4064 and NG5-5020.

7. REFERENCES

Cash, W., 1996. *Applied Optics,* Submitted.
Gallagher, D.G. 1990, *Proc. SPIE*, **1343,** 155.
Gallagher, D.G. 1991, *Proc. SPIE*, San Diego (1991).
Golub, L., *et al.* 1982, *Ap. J.*, **259**, 359.
Golub, L., *et al.* 1989, *Solar Physics,* **122**, 245.
Golub, L., *et al.* 1990, *Nature,* **344**, 842.
Henke, B. L., *et al. 1982*, At. Data Nucl. Data Tables **27**, 1
Hoover, R. B. *et al.* 1990, *Proc. SPIE*, **1343,** 189.
Mewe, R., Lemen, J. R., and van den Oord, G. H. J.: 1985, *Astron. Astrophys. Suppl. Series* **63**, 511
Mewe, R., Lemen, J. R., and van den Oord, G. H. J.: 1986, *Astron. Astrophys. Suppl. Series* **62**, 197
Walker, A.B.C., *et al.* 1988, *Science*, **241**, 1781.
Welch, C.,Physical Science Laboratory @ New Mexico State University.

Third HELSTF Tests

The Experiment

During the last year of this research effort a third test run at HELSTF was done using a modified version of the spherical X-ray telescope. The modifications and day to day activities for this run were carried out by a graduate student (Jason Farmer) with my guidance. The goal of this test was to determine the ultimate resolution of the spherical telescope. This was done by modifying the relay optics to increase the effective focal length of the X-ray telescope 50 meters Effective Focal Length (EFL) to obtain a better sampling of the telescopes point spread function at (.03 arcsec/pixel). The experimental test setup at HELSTF was identical to the previous HELSTF tests except for changes to the telescope. Table I shows the reoptimized telescope angles and the new relay optics for the 50 meter EFL design. The aperture of the telescope was closed down to a 5X5 mm size to further reduce aberrations.

Table I Spherical Telescope Parameters (50 meter EFL design)

Element mm)	Radius(m)	Separation(mm)	Angle (deg)	Comment
Sphere 1	+241400.	0.	1.95299	Focus in X direction
Sphere 2	+218700.	300.	1.94607	Focus in Y direction
Sphere 3	+434900.	300.	2.00110	Correct in X direction
Sphere 4	+380580.	300.	1.96157	Correct in Y direction
Relay	-2000.	2102..3	1.36659	Y direction relay optic
Relay	+750.	36.6	2.12365	X direction relay optic
Plane	∞		na	focal plane

A tolerance analysis on the redesign revealed that angle errors as little as 15 arcsec were enough to degrade the focus quality of the telescope beyond acceptable limits for on axis rays. The alignment constraints can be dramatically relaxed by mounting both the relay optics and the CCD focal plane assembly on a 3-dimensional positioning device. By changing the position of the relay optics relative to the prime focus (image from the first four optics), one can effectively introduce changes to the graze angles of the relay optics. The positioning stage essentially operates as a focusing knob. These slight angle changes can then be used to correct for the alignment errors in the first four optics as well as the relay optics. This corrective measure, while very useful in terms of demonstrating the resolving power of the system and obtaining useful data, is not the optimum solution because the refocused telescope has a smaller focused field of view than one without any misalignments. A more elegant setup would have the mirrors mounted on stages allowing an angle correction before fixing them in place.

Image Data

In this experiment we imaged a back illuminated stainless steel mask with four parallel apertures 1.2 X 25 mm (0.8 X 17 arcsec). The raw image showing the best detail of the mask is shown in figure 1. The three slits are well resolved and the fourth appears to be not illuminated. Unfortunately, the telescope performance is not constant across the field of view. High resolution imaging is only attained in a portion of the field of view. We refer to the high resolution region of the focal plane as the sweet spot. In a perfectly aligned telescope, the "sweet spot" would lie in the center of the CCD detector, but misalignments of as little as 15 arcsec of the primary mirrors can move the sweet spot completely out of the field and off the CCD.

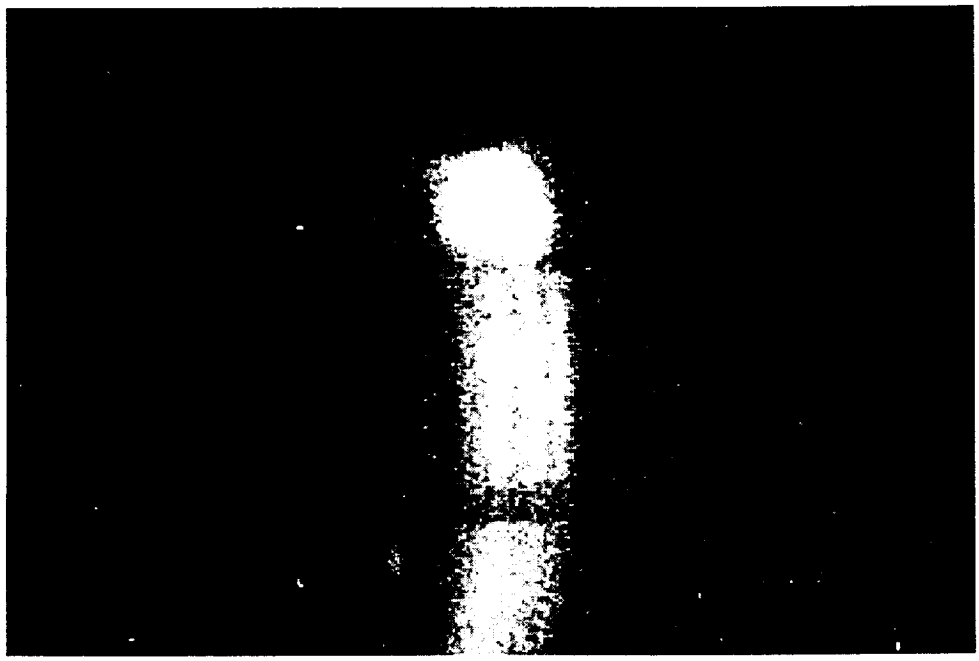

Figure 1: This is an image of the stainless steel mask attached to the annulus of the Wolter telescope being used as a collimator. The mask has four slits, 1.2 X 25 mm in size, and is at a distance of 300 meters. This image was used to define the resolution of the spherical telescope.

Instrument Resolution Analysis

We determined the point spread function of the telescope from the image in figure 1. A histogram across a small section of the image, a few pixels, was computed. The histogram represents an intensity plot of the image of the bars produced by the telescope in one dimension. A 1-D model of the telescope PSF was convolved with a simulated image of the bars and compared to the intensity plot from figure 1.

We modeled the point spread function of the telescope as a two part gaussian where one function represented the core of the image and the other the wings. The intensity profile of the slits were modeled with a boxcar intensity profile. To obtain a reasonable fit to the data, the effects of intensity variations across the image had to be taken into account. These intensity variations are most likely due to imaging the electron density variations

on the anode of the X-ray source since both the mask and source would be in approximately the same focus at 300 meters. To account for this, the box car function for each slit was allowed to vary in height (intensity) to provide a better match. The slit profiles were then convolved with the two element gaussian function where the 1σ widths of the two gaussian functions were allowed to vary. Figure 2 shows the best, minimum sigma, fit of the model to the data.

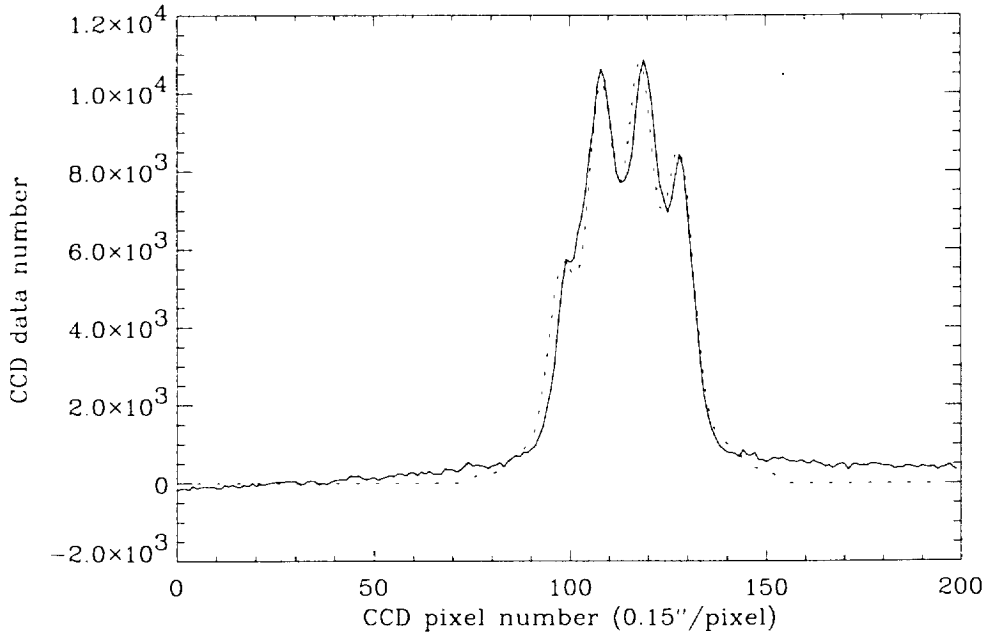

Figure (2): The solid line is the intensity data from the image in figure 1. The dashed line represents the best fit model to the data.

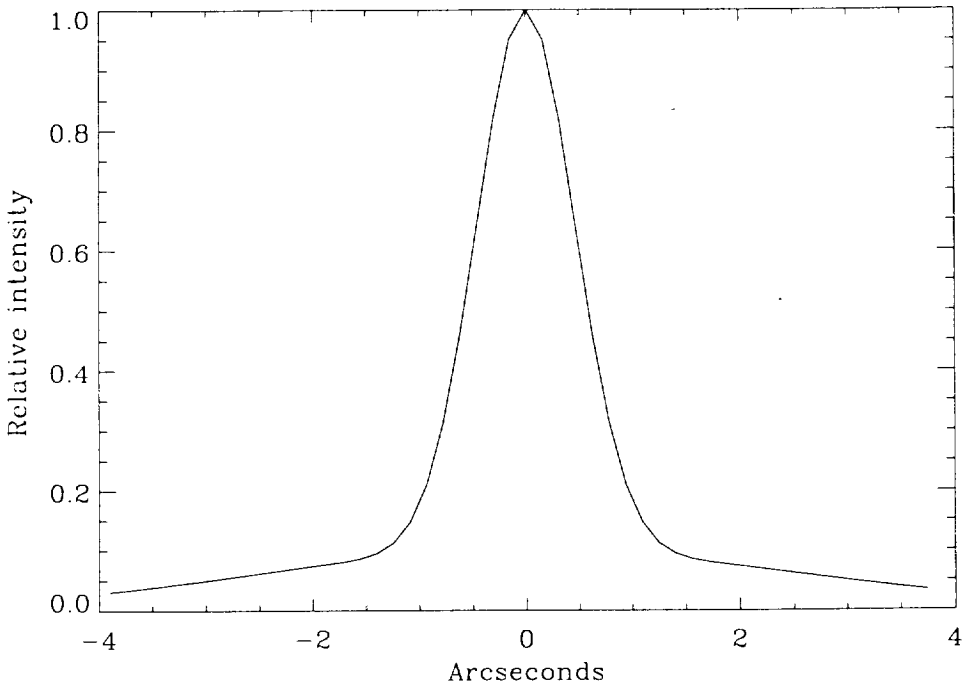

Figure 3: Best fit point spread function as determined from fit to data in figure 2.

Figure 3 shows the point spread function derived for the data in figure 2. The minimum sigma of the best fit gaussian core was 2.1 pixels. The spherical telescope has an EFL of 50 meters and the CCD has 27X27μm pixels giving 0.15 arcseconds per pixel or a 1σ width of 0.31 arcseconds. Applying a resolution criteria that two point sources must be separated by their half energy width (separation = 1.349σ) then the resolution is 0.42 arcseconds. If two point sources are separated by there FWHM (separation = 2.345σ) then the resolution is 0.73 arcseconds. Applying standard resolution criteria to X-ray optics typically leads to invalid results due to scattering from a cylindrical optic, but in the case of the all spherical telescope the optics the scattering is confined to the two orthogonal planes defined by the crossed optics. So scattering form a point source is confined into a fine cross at the focal plane and does not contribute significantly to the increase in diameter of the encircled energy.

Conclusion

We have demonstrated that sub-arcsecond imaging can indeed be achieved using spherical optic at grazing incidence. Further more, we have shown that with standard optical polishing techniques, spheres can be polished to extremely smooth tolerances resulting in low scatter in the x-ray. While the throughputs are low for the spherical telescope designs demonstrated, there are applications in solar physics where these designs will yield an adequate signal to noise. Further work is needed in the study of making nested spherical telescope designs, similar to the manner in which Wolter

telescope are nested. X-ray interferometery becomes a possibility using two 1-D spherical telescopes. If the extreme care that is applied to polishing aspherical optics would be applied to polishing spheres, spherical surfaces approaching $\lambda/1000$ @ 6328 Å and <2 Å RMS would be possible allowing for X-ray interferometery. This work was supported by NASA grant NAGW-4064.